Identification of a widespread Kamchatkan tephra: a middle Pleistocene tie-point between Arctic and Pacific paleoclimatic records

Vera Ponomareva[1], Maxim Portnyagin[2,3], Alexander Derkachev[4], Olaf Juschus[5], Dieter Garbe-Schönberg[6], and Dirk Nürnberg[2]

[1] *Institute of Volcanology and Seismology, Petropavlovsk-Kamchatsky, Russia*

[2] *Helmholtz Centre for Ocean Research Kiel (GEOMAR), Kiel, Germany*

[3] *V.I. Vernadsky Institute of Geochemistry and Analytical Chemistry, Moscow, Russia*

[4] *V.I.Il'ichev Pacific Oceanological Institute, Vladivostok, Russia*

[5] *Eberswalde University of Sustainable Development, Eberswalde, Germany*

[6]*Institute of Geoscience, Christian-Albrechts-University of Kiel, Kiel, Germany*

Corresponding author: Vera Ponomareva

Institute of Volcanology and Seismology, Piip Blvd 9, Petropavlovsk-Kamchatsky, 683006, Russia

E-mail: vera.ponomareva1@gmail.com

Abstract

Very few age controls exist for Quaternary deposits over the vast territory of the East Russian Arctic, which hampers dating of major environmental changes in this area and prevents their correlation to climatic changes in the Arctic and Pacific marine domains. We report a newly identified ~177 ka old Rauchua tephra, which has been dispersed over an area of >1,500,000 km^2 and directly links terrestrial paleoenvironmental archives from Arctic Siberia with marine cores in the northwest Pacific, thus permitting their synchronization and dating. The Rauchua tephra can help to identify deposits formed in terrestrial and marine environments during the oxygen isotope stage 6.5 warming event. Chemical composition of volcanic glass from the Rauchua tephra points to its island-arc origin, while its spatial distribution singles out the Kamchatka volcanic arc as a source. The Rauchua tephra represents a previously unknown, large (magnitude >6.5) explosive eruption from the Kamchatka volcanic arc.

1. Introduction

Establishing precise correlations between distant paleoenvironmental archives is important for resolving the spatial and temporal complexity of past climatic changes. Tephra layers from large explosive eruptions have proved to work as excellent isochrones directly linking marine and terrestrial depositional successions and allowing an evaluation of the synchronicity of abrupt climate changes [e.g., *Davies et al.,* 2008]. Once dated, a tephra layer provides age control for all other sections where it has been geochemically identified. Some tephras have been recently found at distances of more than eight thousand kilometers from their source [*Jensen et al.,* 2012], which attests to the potential of tephra for correlation of distant sites. In addition, tephra correlations permit estimates of tephra volumes, which in turn may serve as a basis for evaluating magma output and volcanic gas flux through time as well as contribute to hazard assessment.

Numerous distal tephra layers have been reported over northeast Asia and surrounding seas (Fig. 1) both in terrestrial and marine environments [*Kotov,* 1998; *Nürnberg and Tiedemann,* 2004;

Juschus et al., 2007]. To date, however, only one tephra associated with the Kurile Lake caldera-forming eruption ~8.4 cal ka BP has been reliably correlated between the source in South Kamchatka, cores in the Okhotsk Sea, and distal sites on the Asian mainland (Fig. 1) [*Ponomareva et al.*, 2004; Derkachev et al., 2012]. Dispersal areas and sources for many other distal tephras are not yet constrained which hampers their usage for dating and correlation of distant paleoclimatic archives. This paper reports new data on the geochemical correlation of a middle Pleistocene tephra from Kamchatka over an area of >1,500,000 km^2 and discusses its potential as a marker for the oxygen isotope (MIS) 6.5 warming event in northeast Asia and adjacent seas. Wide dispersal of this tephra suggests an earlier unknown explosive eruption from the Kamchatka volcanic arc, which may rank within the Earth's largest eruptions.

2. Sample localities for the Rauchua marker tephra

A volcanic ash of unique composition, which we label the Rauchua tephra, was identified in two terrestrial sites in the East Russian Arctic and two marine cores in the northwest Pacific (Fig. 1). The sites are: (1) the Rauchua outcrop on the Eastern Siberian Sea coast, (2) core Lz1024 in the El'gygytgyn Lake (Chukotka); (3) core SO201-2-81KL (Bering Sea), and (4) core SO201-2-40KL (northwest Pacific) (Table 1 of the auxiliary material).

(1) The Rauchua outcrop (Fig. 2) was originally described and sampled by *Kotov* [1998]. The ~6 km long coastal bluff exposes a carbon-rich permafrost sequence, typical for the Arctic Siberia and comprised of massive silts interlayered with lake deposits and peats [*Schirrmeister et al.*, 2011]. The sequence records two cold climate phases with the formation of silts, and three warmer phases with the formation of thermokarst lakes due to permafrost thaw [*Kotov*, 1998]. A 1-10 cm thick layer of white fine ash was described in many subsections along the outcrop, either within the middle peat layer or within the lower silt, 30-50 cm below the peat (Fig. 2, subsections 1 and 2, respectively). The analyzed sample "Rauchua" comes from below the peat.

Radiocarbon dates on twigs and bulk peats from the Rauchua sequence split into two populations: (1) three dates from the upper lacustrine deposits are early Holocene [*Kotov*, 1998], and (2) ten dates from all the other layers are infinite (beyond the range of ^{14}C method, ~50 ka) [*Anderson and Lozhkin*, 2002]. Pollen data for the middle lacustrine package (Fig. 2) point to a warmer-than-present climate [*Anderson and Lozhkin*, 2002]. The whole sequence, except for its Holocene cover, has been related to the late Pleistocene [*Kotov*, 1998], more precisely, to the first half of the Karginsky interstadial [*Anderson and Lozhkin*, 2002] traditionally assigned to MIS 3 [*Astakhov*, 2013].

(2) El'gygytgyn Lake is located ~330 km southeast from the Rauchua site (Fig. 1). It has been cored several times since 1998 with a major ICDP core taken in 2009 [*Melles et al.*, 2012]. The pilot cores were integrated into the ICDP Site 5011 record, which spans the past 3.6 million years. The age-depth model for the composite site was derived from the systematic tuning of various proxies to the Northern hemisphere insolation and the marine oxygen isotope stack [*Melles et al.*, 2012]. Eight visible tephra layers have been found in the composite core [*Nowaczyk et al*., 2013]. Sample Lz1024-EL2, obtained from a pilot core in 2003 (Table 1 of the auxiliary material), comes from the second layer from the top [*Juschus et al.*, 2007]. The age of this tephra (labeled T1) was estimated at ~177 ka [*Nowaczyk et al*., 2013], and it falls into the MIS 6.5 warm phase [*Frank et al*., 2012].

(3) In core SO201-2-81KL (Bering Sea) (Fig. 1) a layer of fine ash coded SR6 occurs at a depth of 861.5-862.5 cm [*Dullo et al*., 2009]. Correlation of this core to the nearby core SO201-2-85KL with the established age-depth model [*Dullo et al.*, 2009; *Riethdorf et al.*, 2012] allows us to infer that the SR6 tephra was deposited prior to 160 ka BP.

(4) In core SO201-2-40KL (northwest Pacific) a ~10 cm thick tephra coded WP14 occurs at a depth of 704.5-714.5 cm and is composed of fine to medium sand (Fig. 1; Table 1 of the auxiliary material) [*Dullo et al*., 2009].

3. Rauchua glass composition

All samples are dominated by colorless volcanic glass with typical bubble-wall appearance and fluidal texture (Fig. 3a). Geochemical characterization of single-glass shards was done with the help of high-precision electron microprobe (EMP) and laser-ablation inductively couple mass-spectrometry (LA-ICP-MS) under conditions described in Text 1 and Table 2 of the auxiliary material. The chemical compositions of volcanic glass obtained at four localities are given in Tables 3 and 4 of the auxiliary material.

Glasses from all the four sites are indistinguishable or very similar in terms of major and trace element composition (Fig. 3b and c) and likely originate from the same volcanic eruption. The glasses have med-K rhyolite near-homogeneous composition (SiO_2= 77.8 ± 0.2 wt.%, K_2O = 2.78 ±0.08 wt.%, 1 s.d., N=103) with a very narrow range of all other major elements, Cl (0.16±0.01 wt.%) and trace elements (Table 1; Fig. 3b and c). Coefficients of similarity [*Borchardt* et al., 1971] for Rauchua glass and those from three other localities calculated for 44 elements are 0.90-0.91, and those for 7 major elements are 0.94-0.96, that confirms the likeness of all the glasses. Formal *t*-test for the case of two-tail distribution and unequal variances (Microsoft Excel) also confirms close similarity of the glasses (Tables 3 and 4 of the auxiliary material). The deviations from equality are rather random and likely reflect occasional and unaccounted-for analytical uncertainties or specific conditions of deposition (e.g., high Cu in SR6 sample resulting from contamination by sulfide precipitates on glass surfaces). Composition of the Rauchua tephra is distinctly different from that of the younger T0 tephra in the El'gygytgyn Lake core (Fig. 3b and c; Table 5 of the auxiliary material); [*Juschus et al.*, 2007].

Trace elements in the Rauchua glass normalized to the composition of the Bulk Silicate Earth [*McDonough and Sun*, 1995] exhibit a zigzag pattern (Fig. 3c) with strong relative enrichment of Large Ion Lithophile Elements (Cs, Rb, Ba), U, As, Sb, Li and Pb relative to similarly incompatible Rare-Earth and High-Field Strength Elements (Ta, Nb, W, Zr, Hf) and low

115 $[Nb(Ta)/La]_N<1$ and $[Nb/Y]_N\sim1$ that suggests an island-arc origin of the Rauchua tephra [e.g.,
116 *Pearce,* 1982; *Noll et al.*, 1996].

117 **4. Rauchua tephra: age, dispersal, source and eruption magnitude**

118 Based on close resemblance of major and trace element composition of glass from Rauchua, T1,
119 SR6 and WP14 tephras we propose that they represent the same tephra. The age of ~177 ka obtained
120 for the Rauchua tephra in the El'gygytgyn Lake core [*Melles et al.,* 2012] can thus be applied to all
121 other sites where this tephra is present. The Rauchua tephra has the greatest thickness (~10 cm) and
122 contains the coarsest material (medium sand) in core SO201-2-40KL (Fig. 1). Dispersal pattern for
123 the Rauchua tephra, thus, points at Kamchatka rather than the Aleutian arc as a source (Fig. 1).

124 The Kamchatka volcanic arc represents the northwest segment of the Pacific Ring of Fire
125 and is highly explosive with the largest number of calderas per unit of arc's length in the world
126 [*Hughes and Mahood*, 2008] and with the dense cluster of nested calderas in the Karymsky volcanic
127 center. A few dated ignimbrites from this area cover a range between ~1,300 and 8.7 ka BP
128 [*Braitseva et al.*, 1995; *Bindeman et al.*, 2010]. There is no exact match for the Rauchua tephra
129 within the age and geochemical data available for this area, however, as yet many local ignimbrites
130 have not been dated or geochemically characterized [e.g., *Leonov and Grib,* 2004]. Geochemical
131 characteristics for the Rauchua tephra are similar to rhyolites from the Karymsky volcanic center
132 which is its most probable source (Fig. 3c).

133 A rough estimate of a minimum volume (Vmin) for the Rauchua tephra is based on a single
134 1-cm isopach [*Legros*, 2000] enclosing all of the studied sites (Fig. 1) and gives Vmin of 49.82 km^3.
135 The magnitude (M) of the Rauchua eruption can be estimated at >6.5 [method by *Pyle*, 2000;
136 assuming pumice density of 0.641 g/cm^3]. The Rauchua tephra thus records a previously unknown
137 M>6.5 eruption from a source likely hidden under nested calderas in the Karymsky volcanic center
138 in eastern Kamchatka. An average tephra thickness of 5 cm observed along the Arctic coast suggests

139 that volume and magnitude estimates for this eruption may increase dramatically when the
140 outermost limits of the Rauchua tephra dispersal are defined.

141 The Rauchua tephra is one of only eight tephras that covered the Far East Russian Arctic
142 with a visible layer during the last 3.6 Ma [*Nowaczyk et al.*, 2013]. This indicates that the Rauchua
143 eruption was a relatively rare and significant volcanic event likely comparable in size to the Earth's
144 largest eruptions, e.g., the Millennium eruption of Changbaishan volcano [*Horn and Schmincke*,
145 2000] or the Kurile Lake caldera-forming eruption (Fig. 1) [*Ponomareva et al*., 2004], and might
146 have had a substantial climatic impact. Remarkably, the Rauchua tephra, as well as some other large
147 tephras (Fig. 1), was dispersed across the westerly polar jet stream, which indicates that its pattern
148 could have been different from the present jet stream.

149 **5. Implications for geochronology and paleoclimate**

150 A few continuous records of late to middle Pleistocene climate change are available from
151 northeast Asia and adjacent seas [e.g., *Nürnberg and Tiedemann*, 2004; *Max et al.*, 2012; *Riethdorf*
152 *et al.*, 2012]. These records exhibit alternating warm and cool phases consistent with other
153 paleoclimatic records from the Northern hemisphere [*Melles et al.*, 2012]. It is still not clear,
154 however, which of these phases have caused the most prominent changes in the landscape over the
155 vast territory of the northeast Siberia, inducing permafrost melting or accumulation of massive silts.
156 In the absence of reliable dating tools, the age of terrestrial deposits beyond the limits of radiocarbon
157 dating remains very uncertain [*Astakhov*, 2013].

158 We propose the Rauchua tephra as a robust marker, which permits the identification of the
159 middle Pleistocene deposits in northeast Asia and adjacent seas, and more specifically, pinpoints the
160 deposits accumulated during the MIS 6.5 warming event. This event was characterized by abrupt
161 changes from glacial to interglacial-type conditions and caused prominent effects over a large area
162 from the Mediterranean to China (strong Mediterranean rainfalls, a sapropel event (S6) in the eastern
163 Mediterranean Sea, changes in monsoon patterns, etc.) [e.g., *Margari et al.*, 2010; *Penaud et al.*

164 *2009*, and refs herein]. It is plausible that this event has left significant, but not yet recognized traces
165 in northeast Asia as well. The Rauchua tephra, thus, will allow an assessment of the regional
166 development of the 6.5 warming event.

167 The whole Rauchua sequence was earlier assigned to late Pleistocene [*Kotov*, 1998; *Lozhkin*
168 *and Anderson*, 2002] as well as many similar permafrost deposits along the Siberian Arctic coastline
169 [*Schirrmeister et al.*, 2011]. Our findings show that these typical carbon-rich permafrost deposits
170 started to form in the middle Pleistocene, well prior to MIS 6.5. No glacial till or marine deposits are
171 present in the Rauchua outcrop indicating that this area has not been glaciated or submerged during
172 the last >177 ka. The middle lacustrine-peat package (Fig. 2) is likely to record the latest pre-
173 Holocene permafrost thaw at this site with the formation of thermokarst lakes and accumulation of
174 the lacustrine-peat deposits. The analyzed Rauchua tephra lies only 30-50 cm below the peat, which
175 suggests that these "warm" Karginsky [*Anderson and Lozhkin*, 2002] sediments formed during MIS
176 5e (Eemian) interglacial (116-130 ka BP [*Melles et al.*, 2012]) rather than during MIS 3 (55-24 cal
177 ka BP). This conclusion is consistent with the results of a recent re-dating of the Karginsky
178 interstadial in western Siberia [*Astakhov*, 2013]. The tephra described by *Kotov* [1998] within the
179 middle peat layer should be significantly younger and likely represents another tephra, which still
180 needs to be analyzed.

181 The Rauchua tephra ensures direct comparison of the marine paleoenvironmental archives in
182 the Bering Sea and northwest Pacific with the well-studied record of the El'gygytgyn lake [*Melles et*
183 *al.*, 2012], which may help to test the synchronicity of the MIS 6.5 warming event in marine and
184 terrestrial environments. The presence of the Rauchua tephra as a visible layer along the Arctic coast
185 and in the northwest Pacific indicates that it may be found as cryptotephra (scattered volcanic glass)
186 yet farther north and east, and thus help to recognize MIS 6.5 sediments in the Arctic and Pacific
187 marine cores and, possibly, even in the North Atlantic, thus permitting a large scale inter-regional

correlations of paleoclimatic records. This study highlights a significant potential of using this and other tephra layers in the western Beringia for precise correlations of distant records.

Acknowledgements. The sample from Rauchua bluff came from the late A.N. Kotov and was kindly provided by A.V. Lozhkin; samples from the marine cores were obtained thanks to the German Federal Ministry for Education and Research (BMBF) KALMAR project. The expedition to Lake El´gygytgyn in 2003 was funded by the BMBF grant no. 03G0586A, B. Sample from Odnoboky caldera came from Vladimir Leonov. All the samples were studied thanks to the KALMAR project. We thank Mario Thöner and Ulrike Westernströer for their assistance with electron probe and LA-ICP-MS analyses. Jody Bourgeois' comments, and reviews from two anonymous reviewers helped to significantly improve the text. Publication was possible thanks to the grants from the Otto Schmidt Laboratory and Russian Foundation for Basic Research project 13-05-00346.

References

Anderson, P.M., and A.V. Lozhkin (2002), Late Quaternary vegetation and climate of Siberia and the Russian Far East (palynological and radiocarbon database), North-Eastern Science Center FEB RAS, Magadan.

Astakhov, V. I. (2013), Pleistocene glaciations of northern Russia – a modern view, *Boreas*, *42*(1), 1–24, doi: 10.1111/j.1502-3885.2012.00269.x.

Bindeman, I.N., et al. (2010), Large-volume silicic volcanism in Kamchatka: Ar-Ar, U-Pb ages and geochemical characteristics of major pre-Holocene caldera-forming eruptions, *J. Volcanol. Geotherm. Res.*, *189*(1-2), 57-80.

Borchardt, G.A., M.E. Harward, and R.A. Schmitt (1971), Correlation of volcanic ash deposits by activation analysis of glass separates, *Quat. Res.*, *1*, 247-260.

211 Braitseva, O.A., I.V. Melekestsev, V.V. Ponomareva, and L.D. Sulerzhitsky (1995), The ages of
212 calderas, large explosive craters and active volcanoes in the Kuril-Kamchatka region, Russia,
213 *Bull. Volcanol.*, *57*, 383-402.
214 Davies, S.M., S. Wastegård, T.L. Rasmussen, S.J. Johnsen, J.P. Steffensen, K.K. Andersen, and A.
215 Svensson (2008), Identification of the Fugloyarbanki tephra in the NGRIP ice-core: a key tie-
216 point for marine and ice-core sequences during the last glacial period, *J. Quat. Sci.*, *23*, 409-414.
217 Derkachev, A.N. et al. (2012), Characteristics and ages of tephra layers in the central Okhotsk Sea
218 over the last 350 kyr, *Deep-Sea Res., Part II*, 61-64, 179-192.
219 Dullo, C., B. Baranov, and Cvd Bogaard (2009), RV Sonne Fahrtbericht, Cruise Report SO201-2:
220 KALMAR (Kurile-Kamchatka and Aleutian Marginal Sea-Island Systems): Geodynamic and
221 Climate Interaction in Space and Time. IFM-GEOMAR Report 35: http://www.ifm-
222 geomar.de/index.php?id=publikationen
223 Frank, U., N. R. Nowaczyk, P. Minyuk, H. Vogel, P. Rosén, and M. Melles (2012), A 350 kyr
224 record of climate change from Lake El'gygytgyn, Far East Russian Arctic: refining the pattern of
225 climate modes by means of cluster analysis: *Clim. Past Discuss.*, v. 8, p. 5109–5132,
226 doi:10.5194/cpd-8-5109-2012
227 Horn, S., and H. U. Schmincke (2000), Volatile emission during the eruption of Baitoushan volcano
228 (China/North Korea) ca. 969 AD, *Bull. Volcanol.*, *61*, 537–555.
229 Hughes, G.R., and G.A. Mahood (2008), Tectonic controls on the nature of large silicic calderas in
230 volcanic arcs. *Geology*, *36*, 627–630.
231 Jensen, B.J., S. Pyne-O'Donnell, G. Plunkett, D.G. Froese, P. Hughes, J.R. Pilcher, and V.A. Hall
232 (2012), Intercontinental distribution of an Alaskan volcanic ash, Abstract V43B-2832 of the
233 AGU Fall Meeting, San Francisco, Dec 3-7, 2012.

234 Juschus, O., F. Preusser, M. Melles, and U. Radtke, (2007), Applying SAR-IRSL methodology for
235 dating fine-grain sediments from Lake El'gygytgyn, northeastern Siberia, *Quat. Geochronol., 2*,
236 187-194.
237 Kaplina, T.N. (2011), Drevnie alasnye kompleksy severnoi Yakutii (Ancient alas complexes of
238 northern Yakutia) (Part 1): *Cryosphera Zemli (Cryosphere of the Earth), XV*(2), 3-13 (In
239 Russian).
240 Kotov, A.N. (1998), Alasny i ledovy komplexy otlozhenii Severo-zapadnoi Chukotki (Alas and ice
241 complexes of the northwestern Chukotka deposits): *Cryosphera Zemli (Cryosphere of the Earth)*,
242 *II*(1), 11-18 (In Russian).
243 Legros, F. (2000), Minimum volume of a tephra fallout deposit estimated from a single isopach, *J.*
244 *Volcanol. Geotherm. Res., 96*, 25–32.
245 Leonov, V.L., and E.N. Grib (2004), Strukturnye pozicii I vulkanism chetvertichnyh calder
246 Kamchatki (The structural position and volcanism of the Quaternary calderas, Kamchatka),
247 Vladivostok, Dalnauka publisher (In Russian).
248 Margari, V., L.C. Skinner, P.C. Tzedakis, A. Ganopolski, M. Vautravers, and N. J. Shackleton
249 (2010), The nature of millennial-scale climate variability during the past two glacial periods, *Nat.*
250 *Geosci., 3*, 127-131.
251 Max, L. et al. (2012), Sea surface temperature variability and sea-ice extent in the subarctic
252 northwest Pacific during the past 15,000 years, *Paleoceanography, 27*, PA3213, doi:
253 10.1029/2012PA002292
254 McDonough, W.F., and S.-s. Sun (1995), The composition of the Earth, *Chem. Geol., 120*, 223-253,
255 doi: 10.1016/0009-2541(94)00140-4.
256 Melles, M. et al. (2012), 2.8 Million years of Arctic climate change from Lake El'gygytgyn, NE
257 Russia. *Science, 337*, 315-320.

Noll Jr., P. D., H. E. Newsom, W. P. Leeman, and J. G. Ryan (1996), The role of hydrothermal fluids in the production of subduction zone magmas: Evidence from siderophile and chalcophile trace elements and boron, *Geochim. Cosmochim. Acta, 60*(4), 587-611.

Nowaczyk, N. R. et al. (2013), Chronology of Lake El'gygytgyn sediments, *Clim. Past Discuss., 9*, p. 3061–3102, doi:10.5194/cpd-9-3061-2013.

Nürnberg, D., and R. Tiedemann (2004), Environmental change in the Sea of Okhotsk during the last 1.1 million years. *Paleoceanography, 19*, PA4011.

Pearce, J. A. (1982), Trace element characteristics of lavas from destructive plate boundaries, in Andesites, edited by R. S. Thorpe, p.p. 525-548, John Wiley & Sons.

Penaud, A., F. Eynaud, J.L. Turon, S. Zaragosi, B. Malaizé, S. Toucanne, and J.F. Bourillet (2009), What forced the collapse of European ice sheets during the last two glacial periods (150 ka BP and 18 ka cal BP)? Palynological evidence, *Palaeogeogr. Palaeocl., 281*, 66–78.

Ponomareva, V.V., P.R. Kyle, I.V. Melekestsev, P.G. Rinkleff, O.V .Dirksen, L.D. Sulerzhitsky, N.E. Zaretskaia, and R. Rourke (2004), The 7600 (14C) year BP Kurile Lake caldera-forming eruption, Kamchatka, Russia: stratigraphy and field relationships, *J..Volcanol. Geotherm. Res.*, *136*, 199–222.

Preece, S.J., N.J.G. Pearce, J.A. Westgate, D.G. Froese, B.J.L. Jensen, and W.T. Perkins (2011), Old Crow tephra across eastern Beringia: a single cataclysmic eruption at the close of Marine Isotope Stage 6: *Quat. Sci. Rev., 30*, 2069–2090.

Pyle, D.M. (2000), Sizes of volcanic eruptions, in Encyclopedia of volcanoes, edited by H. Sigurdsson, B. Houghton, H. Rymer, J. Stix, S. McNutt, pp. 263–269,Academic Press.

Riethdorf, J.-R., Nüernberg, D., Max, L., Tiedemann, R., Gorbarenko, S. A., and M. I. Malakhov (2012), Millennial-scale variability of marine productivity and terrigenous matter supply in the western Bering Sea over the past 180 kyr, *Clim. Past Discus., 8*, 6135–6198.

Schirrmeister, L. et al. (2011), Sedimentary characteristics and origin of the Late Pleistocene Ice Complex on north-east Siberian Arctic coastal lowlands and islands - A review, *Quat. Int. 241*, 3-25.

FIGURE CAPTIONS

Fig. 1. Location of the Rauchua tephra sites and its minimum outline (solid line); with Old Crow (~124 ka) [*Preece et al.*, 2011] and Kurile Lake (KO, ~8.4 ka) [*Ponomareva et al.*, 2004] tephras outlines (dashed) for comparison. Karymsky volcanic center is shown with the star. Some other sites with the MIS 5e (Eemian) interglacial deposits according to *Brigham-Grette et al*. (2001), *Kaplina* (2011), and *Schirrmeister et al.* (2011). Long axis of the Rauchua tephra outline is ~1800 km.

Fig. 2. Eastern part of the Rauchua outcrop (modified from *Kotov* [1998]). The outcrop exhibits two massive silt units with ice wedge casts; three packages of lacustrine deposits interlayered or capped with peat; and modern soil. Tephra is shown with black (in silt) or white (in peat) dashed line. Numbers 1 and 2 show position of typical subsections discussed in the text.

Fig. 3. Composition of Rauchua tephra: a. Backscattered electron image of Rauchua tephra (Rauchua outcrop); b. K_2O-SiO_2 plot showing composition of Rauchua and T0 tephra glass against that of Pleistocene Kamchatka ignimbrites and tephras analyzed thus far; c. Plot of trace element composition of Rauchua and T0 tephras normalized to Bulk Silicate Earth (McDonough and Sun, 1995). Composition of rhyolites from Karymsky and Odnoboky calderas and field of all the Kamchatkan tephras (gray shade) is provided for comparison.

Table 1. Average composition of the Rauchua glass

Element	Units	N points	Concentration	1 s.d.
SiO_2	wt%	103	77.78	0.24
TiO_2	wt%	103	0.23	0.07
Al_2O_3	wt%	103	12.41	0.11
FeO	wt%	103	1.15	0.12
MnO	wt%	103	0.06	0.05
MgO	wt%	103	0.20	0.02
CaO	wt%	103	1.19	0.03
Na_2O	wt%	103	4.02	0.16
K_2O	wt%	103	2.78	0.08
P_2O_5	wt%	103	0.02	0.02
F	wt%	49	0.02	0.04
SO_3	wt%	103	0.01	0.01
Cl	wt%	103	0.16	0.01
Total	**wt%**		**100.00**	
Li	ppm	31	24.2	3.0
Sc	ppm	31	6.4	0.5
Ti	ppm	31	1375	59
V	ppm	31	8.3	3.7
Cu	ppm	31	12.3	9.7
Zn	ppm	31	32.1	6.3
Ga	ppm	31	12.6	0.9
As	ppm	20	7.5	2.1
Rb	ppm	31	48.8	4.2
Sr	ppm	31	105	6
Y	ppm	31	23.6	2.3
Zr	ppm	31	166	16
Nb	ppm	31	3.23	0.23
Mo	ppm	20	2.59	0.34
Sb	ppm	20	0.54	0.08
Cs	ppm	20	2.19	0.26
Ba	ppm	31	618	52
La	ppm	31	12.1	1.0
Ce	ppm	31	24.9	2.2
Pr	ppm	31	3.21	0.20
Nd	ppm	31	13.3	0.8
Sm	ppm	31	3.06	0.25
Eu	ppm	31	0.63	0.05
Gd	ppm	31	3.04	0.34
Tb	ppm	31	0.52	0.05

Dy	ppm	31	3.56	0.38
Ho	ppm	31	0.79	0.07
Er	ppm	31	2.51	0.25
Tm	ppm	31	0.38	0.05
Yb	ppm	31	2.89	0.31
Lu	ppm	31	0.46	0.05
Hf	ppm	31	4.45	0.51
Ta	ppm	31	0.28	0.03
W	ppm	20	0.44	0.17
Pb	ppm	31	9.66	0.91
Th	ppm	31	3.08	0.31
U	ppm	31	1.55	0.15

Note: The composition represents an average from all analyses of single glass shards obtained at four localities. Major elements were analysed by electron microprobe, trace elements - by LA-ICP-MS. The analytical procedure is described in Data Repository Methods

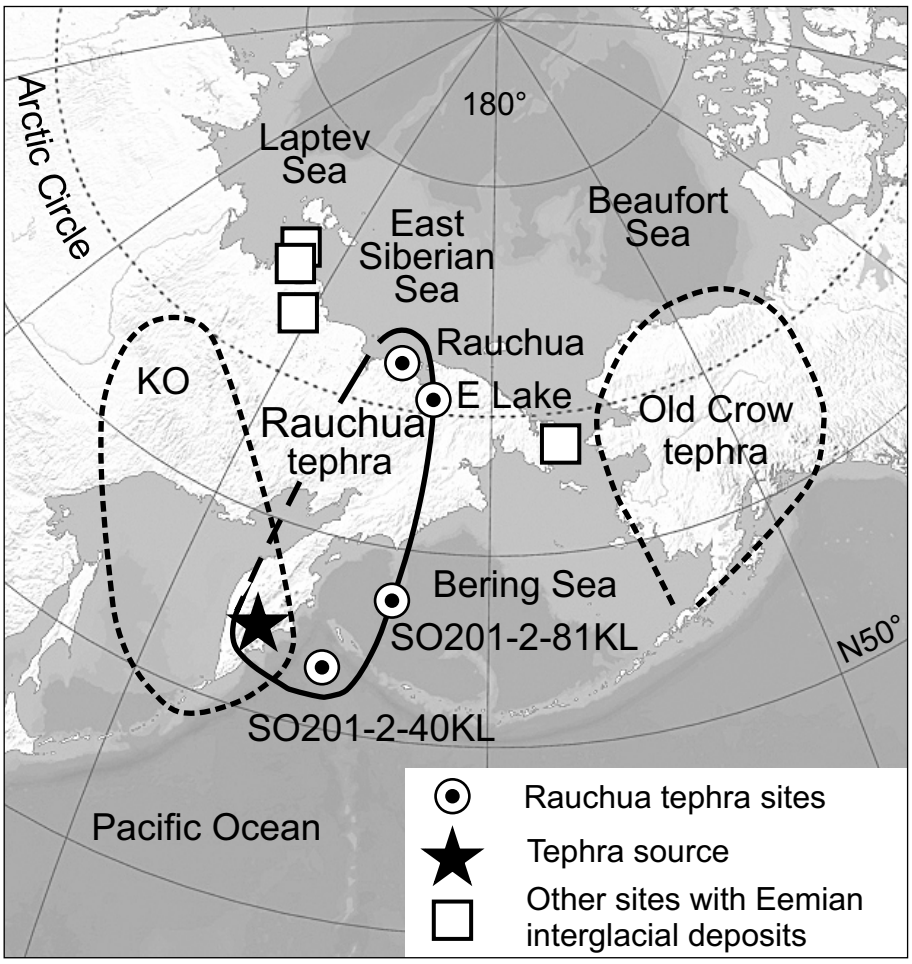
Arctic Circle
180°
Laptev Sea
East Siberian Sea
Beaufort Sea
Rauchua
E Lake
KO
Rauchua tephra
Old Crow tephra
Bering Sea
SO201-2-81KL
SO201-2-40KL
N50°
Pacific Ocean
Rauchua tephra sites
Tephra source
Other sites with Eemian interglacial deposits

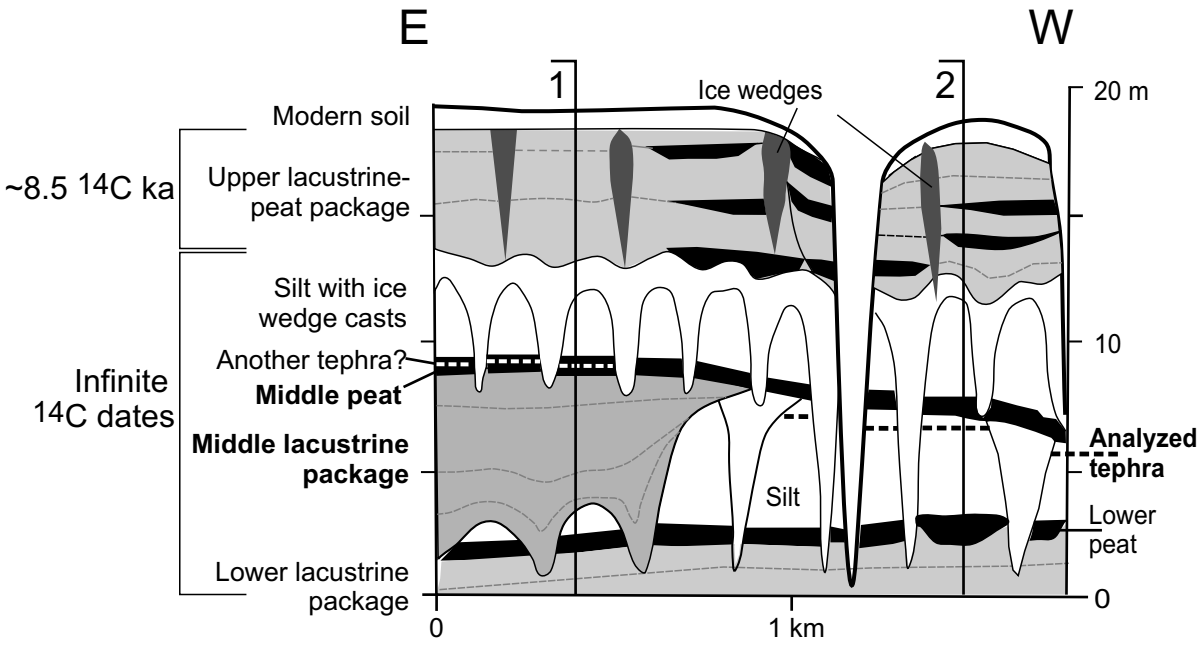
E
W
1
2
Ice wedges
20 m
Modern soil
~8.5 14C ka
Upper lacustrine-peat package
Silt with ice wedge casts
Another tephra?
Infinite 14C dates
Middle peat
Middle lacustrine package
Silt
Analyzed tephra
Lower peat
Lower lacustrine package
10
0
0
1 km

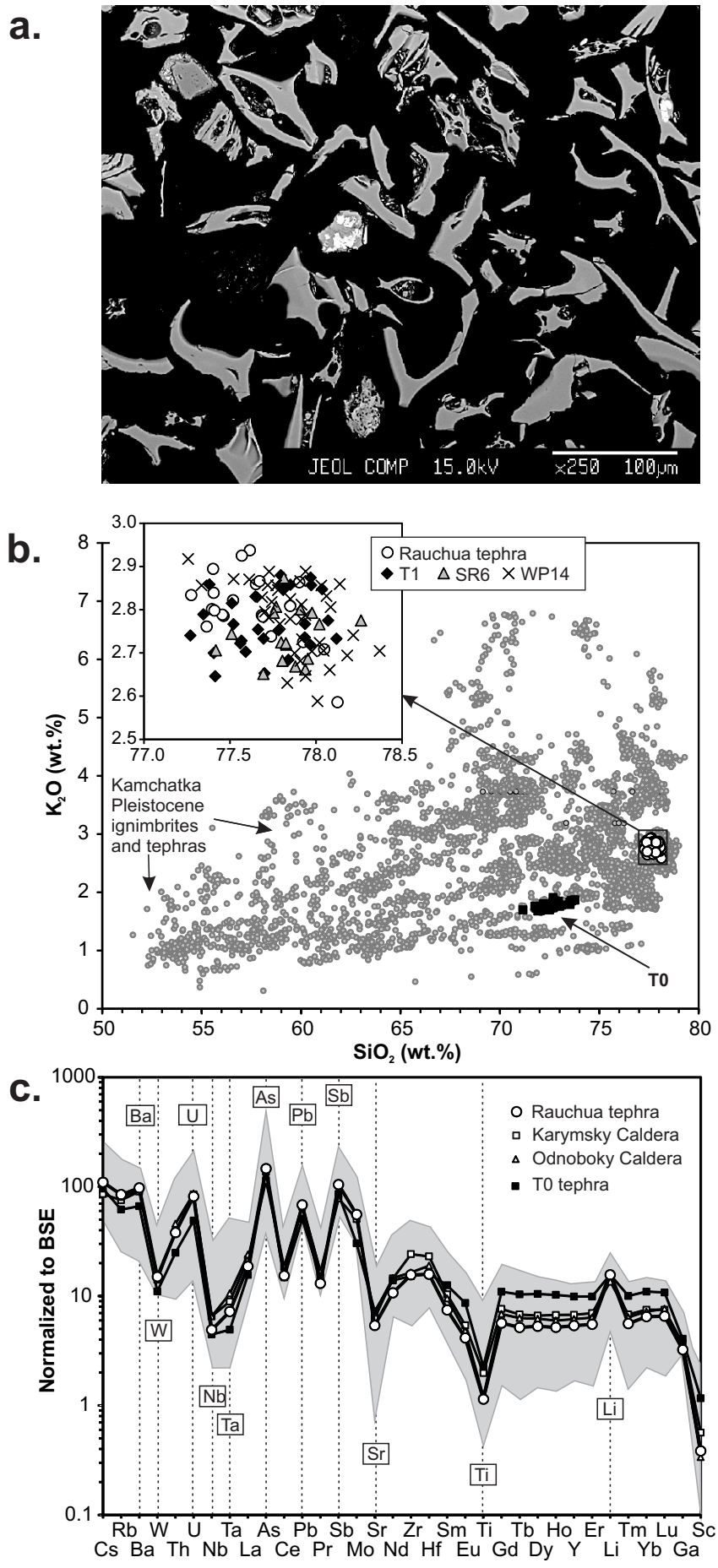
a.
JEOL COMP 15.0kV ×250 100μm
b.
Rauchua tephra
T1 SR6 WP14
Kamchatka
Pleistocene
ignimbrites
and tephras
T0
K2O (wt.%)
SiO2 (wt.%)
c.
Rauchua tephra
Karymsky Caldera
Odnoboky Caldera
T0 tephra
Normalized to BSE
Ba U As Pb Sb W Nb Ta Sr Ti Li
Rb W U Ta As Pb Sb Sr Zr Sm Ti Tb Ho Er Tm Lu Sc
Cs Ba Th Nb La Ce Pr Mo Nd Hf Eu Gd Dy Y Li Yb Ga

Ponomareva et al. (2013) GRL

Auxiliary material, Text01. Methods: Details of the EMP and LA-ICP-MS settings and data processing

Volcanic glass was analyzed using JEOL JXA 8200 electron microprobe equipped with five wavelength dispersive spectrometers including 3 high-sensitivity ones (2 PETH and TAPH) at GEOMAR (Kiel). The analytical conditions for glasses were 15 kV accelerating voltage, 6 nA current and 5 μm electron beam size. Counting time was 5/10 s (peak/background) for Na, 20/10s for (Si, Al, Fe, Mg, Ca), 30/15 s for K, Ti, Cl, S and 40/20 s for Mn and F. Basaltic glass (USNM 113498/1 VG-A99) for Ti, Fe, Mg, Ca, P, rhyolitic glass (USNM 72854 VG568) for Si, Al, K, scapolite (USNM R6600-1) for Na, S and Cl, all from the Smithsonian collection of natural reference materials [*Jarosevich et al.,* 1980], rhyolitic glass KN-18 [*Mosbah et al.,* 1991] for F and synthetic rhodonite for Mn were used for calibration and monitoring of routine measurements. Two to three analyses of the reference glasses and scapolite were performed at the beginning of analytical session, after every 50-60 analyses and at the end. The data reduction included on-line CITZAF correction [*Armb,* 1995] and small correction for systematic deviations (if any) from the reference values obtained on standard materials. The later correction did not exceed 5 % relative for all elements and allowed to achieve the best possible accuracy of the data and long-term reproducibility. The INTAV intercomparison of electron-beam microanalysis of glass by tephrochronology laboratories [*Kuehn et al.,* 2011] revealed no systematic error for glasses compositions analyzed at GEOMAR lab (coded as lab #12).

During the data reduction we excluded EMP analyses with the totals lower than 93 wt%, which resulted from possible unevenness of sample surface, entrapment of voids or epoxy during analysis of very small glass fragments. The latter has been also identified by unusually high measured chlorine concentrations, which resulted from 3-4 wt% of Cl in the epoxy resin used in the course of this study (Buehler EpoThin). Analyses contaminated by occasional entrapment of crystal phases, usually microlites of plagioclase, pyroxene or Fe-Ti oxides, were identified on the basis of excessive concentrations of Al_2O_3, CaO or FeO (and TiO_2), respectively, compared to the prevailing composition of glasses in every sample. Because volcanic glasses can be hydrated over time during post-magmatic interaction with meteoric or sea water or contain significant but variable amount of H_2O, not completely degassed during eruption, all analyses were then normalized to anhydrous basis. The original totals measured by EMP are given in **Auxiliary materials Tables 3 and 5**.

Trace elements in glasses were analysed by laser ablation – inductively coupled plasma – mass spectrometry (LA-ICP-MS) using a 193nm excimer laser with a large volume ablation cell (ETH Zürich, Switzeland) coupled with a quadrupole-based ICP-MS (Agilent 7500s) at the Institute of Geosciences, CAU Kiel, Germany. *In situ*-microsampling was done with 50 µm pit size and 10 Hz pulse frequency at 8.5 J cm^{-2} fluence. The generated aerosol was transported with 0.75 L min^{-1} He and mixed with 0.6 L min^{-1} Ar prior to introduction into the ICP. The ICP-MS was operated under standard conditions at 1500W and optimized for low oxide formation (typically ThO/Th ≤ 0.4%). The GLITTER software package (Access Macquarie Ltd.) was used for data reduction of the time-resolved measurements. The blank signal was measured 20 s prior to each ablation and used for calculation of the actual detection limits. For sample data integration the time window up to 40 s (depending on size of glass shard) was individually adjusted for each run. Calcium (44 m/z) was used for internal standardization utilizing pre-analyzed data from electron probe microanalysis (EPMA). Mass numbers analyzed for every element are listed in **Auxiliary materials Table 2**. The NIST 612 glass [*Jochum et al.*, 2011] and MPI-DING KL-2G (for Ti) were used for calibration of the integrated raw data and re-analysed in triplicate with every batch of 20 sample acquisitions. International rock glass standards (USGS BCR-2G and MPI-DING glass KL-2G and ATHO-G) [*Jochum et al.*, 2006; *GEOREM*, 2012] have been analysed as unknown samples in one series with glass samples for check of accuracy (**Auxiliary materials Table 2**). Analytical precision of five to ten runs of the standard glasses was <5% for most elements during one session. To exclude analyses contaminated by possible entrapment of crystal phases, additional quality test has been applied by comparing Si and Ti concentrations measured by LA-ICP-MS with those obtained by EMPA on the same glass shard. Analysis was accepted as representative for pure glass if both Si and Ti concentrations measured by LA-ICP-MS and EMP agreed within 20% relative. The final LA-ICP-MS data represent background-subtracted averages which passed the quality test and are given in **Auxiliary materials Tables 4 and 5**.

References

Armb, J.T. (1995) CITZAF: A package of correction programs for the quantitative electron microbeam X-ray analysis of thick polished materials, thin films, and particles. Microbeam Analysis, 4, 177-200.

GeoReM (2012) Geological and Environmental Reference Materials, http://georem.mpch-mainz.gwdg.de/ (accessed by 2012)

Jarosewich, E.J., J.A. Nelen, J.A. Norberg (1980) Reference samples for electron microprobe analysis. Geostandard. Newslett., 4, 43-47.

Jochum, K. P. et al. (2006) MPI-DING reference glasses for in situ microanalysis: new reference values for element concentrations and isotope ratios. Geochem. Geophy. Geosy., 7, Q02008, DOI:10.1029/2005GC001060.

Jochum, K. P., U. Weis, B. Stoll, D. Kuzmin, Q. Yang, I. Raczek, D. E. Jacob, A. Stracke, K. Birbaum, D. A. Frick, D. Günther, and J. Enzweiler (2011), Determination of reference values for NIST SRM 610–617 glasses following ISO guidelines. Geostand. Geoanal. Res., 35(4), 397-429. DOI: 10.1111/j.1751-908X.2011.00120.x

Kuehn, S. C., D. G. Froese, and P.A.R. Shane (2011), The INTAV intercomparison of electron-beam microanalysis of glass by tephrochronology laboratories: Results and recommendations, Quat. Int., 246(1-2), 19-47.

Mosbah, M., N. Metrich, and P.Massiot (1991), PIGME fluorine determination using a nuclear microprobe with application to glass inclusions. Nucl. Instrum. Methods, B58, 227-231.